CHAPTER TEN

Failure Criteria

Failure of fiber-reinforced composites may be caused by fiber buckling, fiber breakage, matrix cracking, delamination, or by a combination of these factors (Fig. 10.1). Local fiber buckling, or microbuckling, reduces the compressive stiffness and strength of the laminate. Microbuckling does not necessarily lead to immediate failure because the surrounding matrix supports the fibers. The properties of the fibers and the matrix greatly affect the onset and magnitude of fiber buckling and the resulting losses in the compressive properties of the laminate.

One of the main roles of the fibers is to carry tensile loads. When dry fibers (with no matrix surrounding them) break, they, of course, can no longer carry tensile loads. When the fibers are embedded in a matrix, the matrix acts as a bridge about the break and transmits the load across the gap created by the breakage as well from the broken to the adjacent fibers. Fiber bridging, as this phenomenon is called, is the main reason that the tensile strengths of unidirectional, continuous fiber-reinforced composites are higher than the tensile strengths of dry fiber bundles.

Matrix cracking frequently occurs in composite laminates. In itself, matrix cracking generally does not result in ultimate failure of a laminate. Nonetheless, matrix cracks have many detrimental effects: they facilitate moisture absorbtion, reduce the matrix-dominated stiffnesses of the laminate and, last but not least, may propagate into the interface between adjacent layers, initiating delamination.

Delamination is a separation of adjacent layers that may be introduced either during manufacture or subsequently by loads applied to the laminate. For example, loads due to transverse impact by an object on the laminate are a frequent cause of delamination. Delamination reduces the bending stiffness and strength as well as the load carrying capability of the laminate under compression. Significantly, under repeated loading the size of the delamination may increase to a critical point. Like the behavior of a crack in metal, once the critical size is reached, the growth of the delamination becomes unstable, leading to a rapid loss of compressive strength.

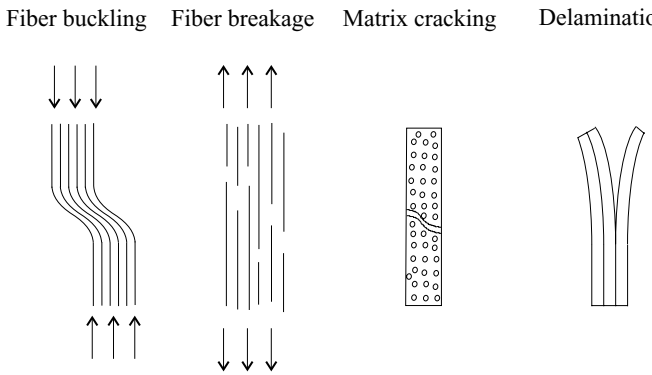

Figure 10.1: Typical failure modes of composites.

Designers would be well served by mechanism-based (physical) theories that would indicate the load at which failure occurs as well as the mode of failure. Although such theories have been proposed,[1,2] none is as yet at the stage where it could be applied in practical engineering design. Instead, frequently, ply–stress-based failure theories are used.[3,4] According to these theories the criterion for failure in any one of the plies is

$$f\,(\sigma_1, \sigma_2, \sigma_3, \tau_{23}, \tau_{13}, \tau_{12}, F_1, F_2, \ldots) \begin{cases} < 1 & \text{no failure} \\ = 1 & \text{failure limit}\,, \\ > 1 & \text{failure} \end{cases} \tag{10.1}$$

where $\sigma_1, \ldots, \tau_{12}$ are the stresses in the ply and $F_1, F_2, \ldots$ are strength parameters. The criterion expressed by Eq. (10.1) is established in every ply, and failure is taken to occur when any one of the plies fails (first-ply failure).

Here, we present three failure criteria for composites based on the aforementioned concept: the quadratic, the maximum stress, and the maximum strain failure criteria. These criteria offer results that are sufficiently accurate for many (but by no means all) problems of practical interest. For this reason, in spite of their shortcomings, they are relevant to the engineer. Nonetheless, the reader is warned to be cognizant of the following significant limits of the criteria listed above:

- Each criterion provides only the load at which first-ply failure occurs, that is, the load at which the linear load-displacement curve first changes (Fig. 10.2). Under the load set that causes first-ply failure, the laminate does not necessarily fail because other undamaged plies can still carry load. As the applied loads

[1] R. F. Gibson, *Principles of Composite Material Mechanics*. McGraw-Hill, New York, 1994, pp. 114–126, 244–249, and 356–367.

[2] S. R. Swanson, *Advanced Composite Materials*. Prentice-Hall, Upper Saddle River, New Jersey, 1997, pp. 91–120, 123–147.

[3] R. E. Rowlands, Strength (Failure) Theories and Their Experimental Correlation. In: *Handbook of Composites*, Vol. 3. G. C. Sih and A. M. Skudra, eds., Elsevier, Amsterdam, 1985, pp. 71–125.

[4] M. N. Nahas, Survey of Failure and Post-Failure Theories of Laminated Fiber Reinforced Composites. *Journal of Composites Technology and Research*, Vol. 8, 138–153, 1986.

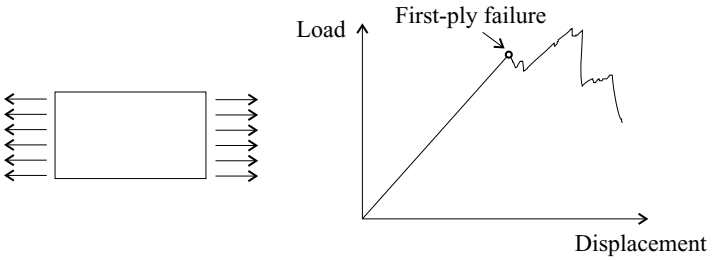

Figure 10.2: Load-displacement curve of a composite part.

are increased beyond those at which first-ply failure occurs, there will be a sequence of ply failures until the load set is reached at which every ply has failed. The loads at ultimate failure may be considerably higher than at first-ply failure. Therefore, criteria based on first-ply failure are conservative.

- None of the criteria sheds light on the failure mechanism or indicates the mode of failure.
- None of the criteria provides acceptable results for every condition of practical interest.
- Each criterion requires data, some of which are difficult to measure.
- Each criterion applies in regions inside the composite away from discontinuities such as holes, cracks, and edges. (Criteria applicable to plates containing a hole or a notch are given in Section 10.4.)

10.1 Quadratic Failure Criterion

The quadratic failure criterion includes stresses up to the second power. In its most general form the quadratic failure criterion states that no failure occurs when the inequality below (Eq. 10.2) is satisfied. This criterion and some of its simplified forms are variously referred to as Tsai-Wu, Hill, or Tsai–Hill failure criterion.

$$\begin{aligned} &F_1\sigma_1 + F_2\sigma_2 + F_3\sigma_3 + F_4\tau_{23} + F_5\tau_{13} + F_6\tau_{12} + \\ &F_{11}\sigma_1^2 + F_{22}\sigma_2^2 + F_{33}\sigma_3^2 + F_{44}\tau_{23}^2 + F_{55}\tau_{13}^2 + F_{66}\tau_{12}^2 + \\ &2(F_{12}\sigma_1\sigma_2 + F_{13}\sigma_1\sigma_3 + F_{14}\sigma_1\tau_{23} + F_{15}\sigma_1\tau_{13} + F_{16}\sigma_1\tau_{12} + \\ &F_{23}\sigma_2\sigma_3 + F_{24}\sigma_2\tau_{23} + F_{25}\sigma_2\tau_{13} + F_{26}\sigma_2\tau_{12} + F_{34}\sigma_3\tau_{23} + \\ &F_{35}\sigma_3\tau_{13} + F_{36}\sigma_3\tau_{12} + F_{45}\tau_{23}\tau_{13} + F_{46}\tau_{23}\tau_{12} + F_{56}\tau_{13}\tau_{12}) < 1, \end{aligned} \tag{10.2}$$

where $\sigma_1, \sigma_2, \ldots, \tau_{12}$ are the components (in the x_1, x_2, x_3 coordinate system) of the stress at the point of interest, that is, the stress that results from the applied loads, and the F's are strength parameters that depend on the material. No failure occurs when the left-hand side of Eq. (10.2) is less then unity. This means that the resultant stress is inside the failure surface (Fig. 10.3, left). On the failure surface (Fig. 10.3, middle), where the stress components are denoted by $\sigma_1^{\mathrm{f}}, \sigma_2^{\mathrm{f}}, \ldots, \tau_{12}^{\mathrm{f}}$.

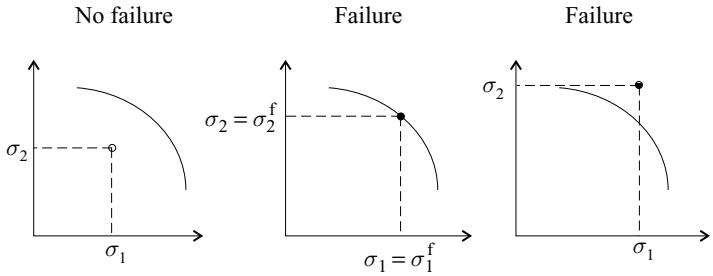

Figure 10.3: Representation of the failure surface when only σ_1 and σ_2 stresses are applied.

Eq. (10.2) is

$$F_1\sigma_1^f + F_2\sigma_2^f + F_3\sigma_3^f + F_4\tau_{23}^f + F_5\tau_{13}^f + F_6\tau_{12}^f + F_{11}\left(\sigma_1^f\right)^2 + F_{22}\left(\sigma_2^f\right)^2 + F_{33}\left(\sigma_3^f\right)^2 + F_{44}\left(\tau_{23}^f\right)^2 + F_{55}\left(\tau_{13}^f\right)^2 + F_{66}\left(\tau_{12}^f\right)^2 + 2\left(F_{12}\sigma_1^f\sigma_2^f + F_{13}\sigma_1^f\sigma_3^f + \cdots + F_{56}\tau_{13}^f\tau_{12}^f\right) = 1. \tag{10.3}$$

The strength parameters must be determined by tests. For generally anisotropic and monoclinic materials, 27 and 17 types of tests are required, respectively. This makes the use of the quadratic failure criterion impractical for structures made of generally anisotropic or monoclinic materials. The criterion becomes more manageable when the material is orthotropic or transversely isotropic. Therefore, in the following the criterion is presented only for these two types of materials.

10.1.1 Orthotropic Material

An orthotropic material has three planes of symmetry (Figs. 2.11 and 2.12). We select the x_1, x_2, x_3 coordinate system with axes perpendicular to these symmetry planes.

First, we consider only the shear–stress component τ_{23} acting in the plane of symmetry (Fig. 10.4). When only τ_{23} acts, and it is in the positive direction, then

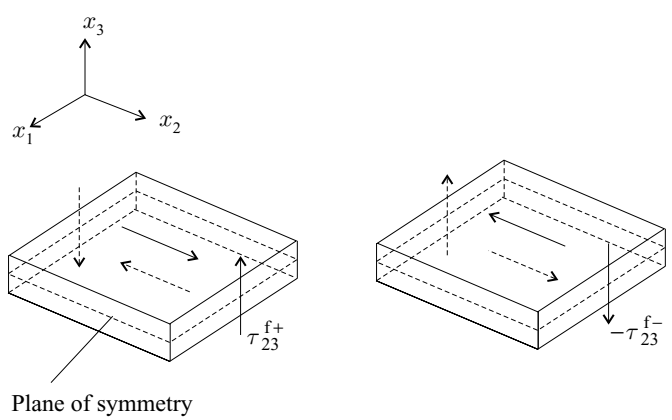

Figure 10.4: The positive and negative shear stresses at failure acting in an orthotropic material; x_1, x_2, and x_3 are perpendicular to the orthotropy planes.

at failure ($\tau_{23} = \tau_{23}^{f+}$) the quadratic failure criterion yields (Eq. 10.3)

$$F_4\tau_{23}^{f+} + F_{44}\left(\tau_{23}^{f+}\right)^2 = 1. \tag{10.4}$$

When only τ_{23} acts in the negative direction, then, at failure ($\tau_{23} = -\tau_{23}^{f-}$) the quadratic failure criterion becomes (Eq. 10.3)

$$-F_4\tau_{23}^{f-} + F_{44}\left(\tau_{23}^{f-}\right)^2 = 1. \tag{10.5}$$

Because of symmetry, the failure stress for positive shear is the same as for negative shear ($\tau_{23}^{f+} = \tau_{23}^{f-}$). The two preceding equations satisfy this condition only if F_4 is zero.

By similar argument it can be shown that F_5, F_6 are zero. Thus, we have

$$F_4 = F_5 = F_6 = 0. \tag{10.6}$$

Next, we apply the normal stresses σ_1, σ_2, σ_3; the shear stresses τ_{12}, τ_{13}; and either a positive or a negative shear stress τ_{23} (Fig. 10.5). For a positive shear stress at failure, $\tau_{23} = \tau_{23}^{f+}$, and we have (Eq. 10.3)

$$\begin{aligned} &F_1\sigma_1^f + F_2\sigma_2^f + F_3\sigma_3^f + F_{11}\left(\sigma_1^f\right)^2 + F_{22}\left(\sigma_2^f\right)^2 + \\ &F_{33}\left(\sigma_3^f\right)^2 + F_{44}\left(\tau_{23}^{f+}\right)^2 + F_{55}\left(\tau_{13}^f\right)^2 + F_{66}\left(\tau_{12}^f\right)^2 + \\ &\qquad 2\left(F_{12}\sigma_1^f\sigma_2^f + F_{13}\sigma_1^f\sigma_3^f + \cdots\right) + \cdots + \\ &+2\left(F_{14}\sigma_1^f + F_{24}\sigma_2^f + F_{34}\sigma_3^f + F_{45}\tau_{13}^f + F_{46}\tau_{12}^f\right)\tau_{23}^{f+} = 1. \end{aligned} \tag{10.7}$$

For a negative shear stress at failure, $\tau_{23} = -\tau_{23}^{f-}$, and Eq. (10.3) gives

$$\begin{aligned} &F_1\sigma_1^f + F_2\sigma_2^f + F_3\sigma_3^f + F_{11}\left(\sigma_1^f\right)^2 + F_{22}\left(\sigma_2^f\right)^2 + \\ &F_{33}\left(\sigma_3^f\right)^2 + F_{44}\left(\tau_{23}^{f-}\right)^2 + F_{55}\left(\tau_{13}^f\right)^2 + F_{66}\left(\tau_{12}^f\right)^2 + \\ &\qquad 2\left(F_{12}\sigma_1^f\sigma_2^f + F_{13}\sigma_1^f\sigma_3^f + \cdots\right) + \cdots + \\ &-2\left(F_{14}\sigma_1^f + F_{24}\sigma_2^f + F_{34}\sigma_3^f + F_{45}\tau_{13}^f + F_{46}\tau_{12}^f\right)\tau_{23}^{f-} = 1. \end{aligned} \tag{10.8}$$

Because of symmetry, the failure stress for positive out-of-plane shear is the same as for negative out-of-plane shear ($\tau_{23}^{f+} = \tau_{23}^{f-}$). This condition, together with

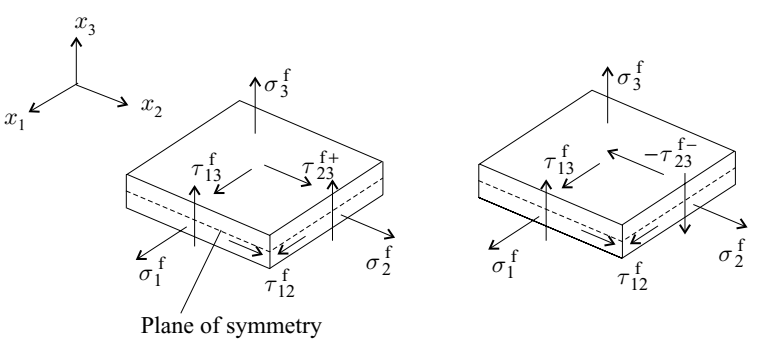

Figure 10.5: The stresses at failure acting on an orthotropic material.

the two preceding equations (Eqs. 10.7 and 10.8), give

$$F_{14} = F_{24} = F_{34} = F_{45} = F_{46} = 0. \tag{10.9}$$

By applying the procedure just given to the other two symmetry planes we find that the following strength parameters are also zero:

$$\begin{aligned} &F_{15} = F_{25} = F_{35} = F_{45} = F_{56} = 0 \\ &F_{16} = F_{26} = F_{36} = F_{46} = F_{56} = 0. \end{aligned} \tag{10.10}$$

For an orthotropic material the quadratic failure criterion (Eq. 10.2) becomes

$$\begin{aligned} &F_1\sigma_1 + F_2\sigma_2 + F_3\sigma_3 + \\ &F_{11}\sigma_1^2 + F_{22}\sigma_2^2 + F_{33}\sigma_3^2 + F_{44}\tau_{23}^2 + F_{55}\tau_{13}^2 + F_{66}\tau_{12}^2 + \\ &\qquad 2(F_{12}\sigma_1\sigma_2 + F_{13}\sigma_1\sigma_3 + F_{23}\sigma_2\sigma_3) < 1. \end{aligned} \tag{10.11}$$

At failure, where the stress components are designated by the superscript f, Eq. (10.11) is

$$\begin{aligned} &F_1\sigma_1^{\mathrm{f}} + F_2\sigma_2^{\mathrm{f}} + F_3\sigma_3^{\mathrm{f}} + F_{11}\left(\sigma_1^{\mathrm{f}}\right)^2 + F_{22}\left(\sigma_2^{\mathrm{f}}\right)^2 + \\ &F_{33}\left(\sigma_3^{\mathrm{f}}\right)^2 + F_{44}\left(\tau_{23}^{\mathrm{f}}\right)^2 + F_{55}\left(\tau_{13}^{\mathrm{f}}\right)^2 + F_{66}\left(\tau_{12}^{\mathrm{f}}\right)^2 + \\ &\qquad 2\left(F_{12}\sigma_1^{\mathrm{f}}\sigma_2^{\mathrm{f}} + F_{13}\sigma_1^{\mathrm{f}}\sigma_3^{\mathrm{f}} + F_{23}\sigma_2^{\mathrm{f}}\sigma_3^{\mathrm{f}}\right) = 1. \end{aligned} \tag{10.12}$$

Noninteraction strength parameters. The noninteraction strength parameters are denoted by $F_1, F_2, F_3, F_{11}, F_{22}, F_{33}, F_{44}, F_{55}, F_{66}$. The values of these parameters are obtained from uniaxial and from shear tests.

To obtain F_1 and F_{11} we subject the material to uniaxial tension and compression in the x_1 orthotropy direction (Table 10.1, top left and middle left). At failure, the stresses are $\sigma_1^{\mathrm{f}} = s_1^+$ and $\sigma_1^{\mathrm{f}} = -s_1^-$, where s is the strength of the material and the superscripts $(+)$ and $(-)$ refer to tension and compression. With these stresses, the quadratic failure criterion gives (Eq. 10.12)

$$F_1 s_1^+ + F_{11}(s_1^+)^2 = 1 \qquad - F_1 s_1^- + F_{11}(s_1^-)^2 = 1. \tag{10.13}$$

Solution of these two equations yields

$$F_1 = \frac{1}{s_1^+} - \frac{1}{s_1^-} \qquad F_{11} = \frac{1}{s_1^+ s_1^-}. \tag{10.14}$$

The strength parameters F_2, F_3, F_{22}, F_{33} are obtained in a similar manner and are given in Table 10.2. The tests to determine $s_2^+, s_2^-, s_3^+, s_3^-$ are illustrated in Table 10.1.

To obtain the strength parameter F_{44} we subject the material to shear τ_{23} in the x_2–x_3 orthotropy plane (Table 10.1, bottom left). Because of material symmetry the failure stress is independent of the direction of the shear stress, and at failure $\tau_{23}^{\mathrm{f}} = s_{23} (= s_{23}^+ = s_{23}^-)$. With this stress, Eq. (10.12) gives

$$F_{44}\left(s_{23}\right)^2 = 1, \tag{10.15}$$

Table 10.1. Tests to determine the strengths of orthotropic materials; σ_1, σ_2, σ_3 are perpendicular to the planes of orthotropy.

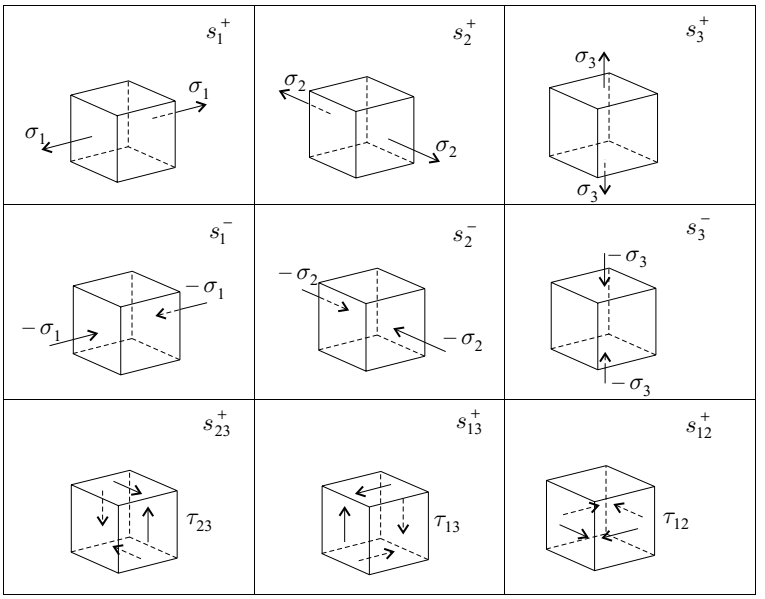

which results in

$$F_{44} = \frac{1}{(s_{23})^2}. \tag{10.16}$$

The strength parameters F_{55}, F_{66} are obtained in a similar manner. These, as well as the other noninteraction strength parameters, are given in Table 10.2.

Interaction strength parameters. The interaction strength parameters F_{12}, F_{13}, and F_{23} can be determined from tests that result in two or more nonzero stress components inside the material. Off-axis uniaxial tests and biaxial tests offer possible means for determining the interaction strength parameters.

Off-axis uniaxial tests. When the interaction strength parameters of orthotropic materials are to be determined by off-axis tests, we take test coupons from each (x_1–x_2, x_2–x_3, and x_1–x_3) orthotropy plane (Fig. 10.6).

Table 10.2. The noninteraction strength parameters in terms of strengths

$F_1 = \frac{1}{s_1^+} - \frac{1}{s_1^-}$	$F_2 = \frac{1}{s_2^+} - \frac{1}{s_2^-}$	$F_3 = \frac{1}{s_3^+} - \frac{1}{s_3^-}$
$F_{11} = \frac{1}{s_1^+ s_1^-}$	$F_{22} = \frac{1}{s_2^+ s_2^-}$	$F_{33} = \frac{1}{s_3^+ s_3^-}$
$F_{44} = \frac{1}{(s_{23})^2}$	$F_{55} = \frac{1}{(s_{13})^2}$	$F_{66} = \frac{1}{(s_{12})^2}$

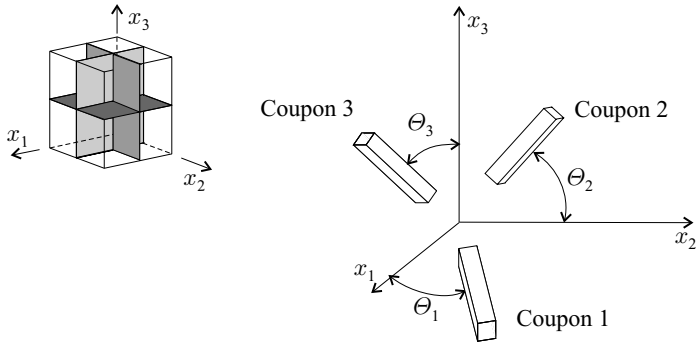

Figure 10.6: Test coupons in the x_1–x_2, x_1–x_3, x_2–x_3 orthotropy planes.

Coupon 1, taken from the x_1–x_2 orthotropy plane, is subjected either to an axial tensile or to an axial compressive stress. At failure the stress is designated by p^{f1}. Superscript 1 indicates Coupon 1. The corresponding stresses in the x_1, x_2 coordinate system are (Eq. 2.182)

$$\sigma_1^{\mathrm{f1}} = p^{\mathrm{f1}} \cos^2 \Theta_1 \qquad \sigma_2^{\mathrm{f1}} = p^{\mathrm{f1}} \sin^2 \Theta_1 \qquad \tau_{12}^{\mathrm{f1}} = p^{\mathrm{f1}} \cos \Theta_1 \sin \Theta_1. \quad (10.17)$$

The angle Θ_1 is shown in Figure 10.6. Substitution of the preceding stresses into Eq. (10.12) results in the expression

$$\begin{aligned} p^{\mathrm{f1}}(F_1 \cos^2 \Theta_1 + F_2 \sin^2 \Theta_1) + \\ (p^{\mathrm{f1}})^2(F_{11} \cos^4 \Theta_1 + F_{22} \sin^4 \Theta_1 + F_{66} \cos^2 \Theta_1 \sin^2 \Theta_1) + \\ (p^{\mathrm{f1}})^2 2F_{12} \cos^2 \Theta_1 \sin^2 \Theta_1 = 1. \end{aligned} \quad (10.18)$$

This equation can be solved for F_{12}. The result is given in Table 10.3. The F_{13}, F_{23} interaction strength parameters are obtained in a similar manner and are also included in Table 10.3.

Biaxial tests. When the interaction strength parameter F_{12} is to be determined from biaxial tests, the specimen is loaded in biaxial tension, resulting in stresses σ_1 and σ_2 (Fig. 10.7). The load is then increased proportionally such that the ratio of the two stresses remains constant. At failure the stresses are denoted by

$$\sigma_1 = \sigma_1^{\mathrm{f(1–2)}} \qquad \sigma_2 = \sigma_2^{\mathrm{f(1–2)}}. \quad (10.19)$$

Table 10.3. The interaction strength parameters obtained from uniaxial tests (orthotropic material). The angles Θ_1, Θ_2, and Θ_3 are shown in Figure 10.6.

$$F_{12} = \frac{1}{2\sin^2 \Theta_1 \cos^2 \Theta_1}\left(\frac{1}{(p^{\mathrm{f1}})^2} - \frac{F_1 \cos^2 \Theta_1 + F_2 \sin^2 \Theta_1}{p^{\mathrm{f1}}} - F_{11} \cos^4 \Theta_1 - F_{22} \sin^4 \Theta_1\right) - \frac{F_{66}}{2}$$

$$F_{23} = \frac{1}{2\sin^2 \Theta_2 \cos^2 \Theta_2}\left(\frac{1}{(p^{\mathrm{f2}})^2} - \frac{F_2 \cos^2 \Theta_2 + F_3 \sin^2 \Theta_2}{p^{\mathrm{f2}}} - F_{22} \cos^4 \Theta_2 - F_{33} \sin^4 \Theta_2\right) - \frac{F_{44}}{2}$$

$$F_{13} = \frac{1}{2\sin^2 \Theta_3 \cos^2 \Theta_3}\left(\frac{1}{(p^{\mathrm{f3}})^2} - \frac{F_3 \cos^2 \Theta_3 + F_1 \sin^2 \Theta_3}{p^{\mathrm{f3}}} - F_{33} \cos^4 \Theta_3 - F_{11} \sin^4 \Theta_3\right) - \frac{F_{55}}{2}$$

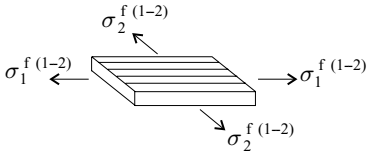

Figure 10.7: Test coupon for biaxial testing in the x_1–x_2 orthotropy plane.

The superscript f refers to the stresses at failure, and the superscript 1–2 identifies the applied biaxial stress components in the x_1–x_2 orthotropy plane. By substituting $\sigma_1^{f(1-2)}$ and $\sigma_2^{f(1-2)}$ into Eq. (10.12), and by setting all other stress components equal to zero, we obtain

$$F_1\sigma_1^{f(1-2)} + F_2\sigma_2^{f(1-2)} + F_{11}\left(\sigma_1^{f(1-2)}\right)^2 + F_{22}\left(\sigma_2^{f(1-2)}\right)^2 + 2F_{12}\sigma_1^{f(1-2)}\sigma_2^{f(1-2)} = 1. \tag{10.20}$$

Equation (10.20) results in

$$F_{12} = \frac{1 - F_1\sigma_1^{f(1-2)} - F_2\sigma_2^{f(1-2)} - F_{11}\left(\sigma_1^{f(1-2)}\right)^2 - F_{22}\left(\sigma_2^{f(1-2)}\right)^2}{2\sigma_1^{f(1-2)}\sigma_2^{f(1-2)}}. \tag{10.21}$$

The other interaction strength parameters, obtained in a similar manner, are

$$F_{ij} = \frac{1 - F_i\sigma_i^{f(i-j)} - F_j\sigma_j^{f(i-j)} - F_{ii}\left(\sigma_i^{f(i-j)}\right)^2 - F_{jj}\left(\sigma_j^{f(i-j)}\right)^2}{2\sigma_i^{f(i-j)}\sigma_j^{f(i-j)}} \quad i,\, j = 1, 2, 3. \tag{10.22}$$

Approximate expressions for the interaction strength parameters. In practice, it is difficult to perform the tests needed to generate the interaction strength parameters F_{ij}. To eliminate the need for these tests, numerous approximate expressions have been proposed for F_{ij}. One of these expressions is obtained by observing that a quadratic equation is characterized by its discriminants. When all but any two of the normal stresses are zero in the failure criterion (Eq. 10.12), the discriminants are

$$\Delta_{ij} = F_{ii}F_{jj} - F_{ij}^2 \quad i,\, j = 1, 2, 3 \quad i \neq j. \tag{10.23}$$

For the quadratic equation to represent a closed domain (which in our case is necessary to ensure that the stresses remain finite), every discriminant must be positive. Thus, from Eq. (10.23) we have

$$-\sqrt{F_{ii}F_{jj}} < F_{ij} < \sqrt{F_{ii}F_{jj}}. \tag{10.24}$$

For convenience, we write

$$F_{ij} = f_{ij}\sqrt{F_{ii}F_{jj}}. \tag{10.25}$$

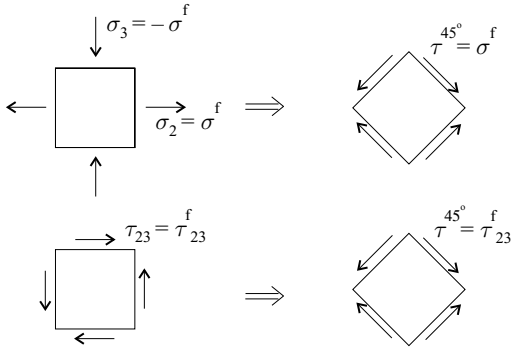

Figure 10.8: Stresses in the x_2–x_3 isotropy plane of a transversely isotropic material.

f_{ij} are constants that may have any value within -1 and $+1$. Tsai and Hahn[5] observed that the quadratic failure criterion for composites reduces to the von Mises quadratic failure criterion for isotropic materials (Section 10.1.3) when $f_{ij} = -0.5$. With this value the interaction strength parameters become

$$F_{12} = -\frac{1}{2}\sqrt{F_{11}F_{22}} \qquad F_{13} = -\frac{1}{2}\sqrt{F_{11}F_{33}} \qquad F_{23} = -\frac{1}{2}\sqrt{F_{22}F_{33}}. \quad (10.26)$$

10.1.2 Transversely Isotropic Material

A transversely isotropic material has three planes of symmetry (Fig. 2.15, page 19). Therefore, the stress parameters, which are zero for an orthotropic material (which also has three planes of symmetry), are also zero for transversely isotropic materials (Eqs. 10.9 and 10.10). In addition, one of the symmetry planes is isotropic. We select this to be the x_2–x_3 plane (Fig. 2.15). Because of isotropy, in this plane the subscripts 2 and 3 are interchangeable, and we can write

$$F_2 = F_3 \qquad F_{22} = F_{33} \qquad F_{13} = F_{12}. \quad (10.27)$$

For the same reason $s_{12} = s_{13}$, and from Table 10.2 (page 417) we have

$$F_{55} = F_{66}. \quad (10.28)$$

We now apply tensile σ_2 and compressive σ_3 stresses of equal magnitude ($\sigma_2 = -\sigma_3$) (Fig. 10.8, top left). At failure, $\sigma_2 = \sigma^f$, $\sigma_3 = -\sigma^f$, and Eq. (10.12) yields

$$F_2\sigma^f - F_3\sigma^f + F_{22}(\sigma^f)^2 + F_{33}(\sigma^f)^2 - 2F_{23}(\sigma^f)^2 = 1. \quad (10.29)$$

By combining Eqs. (10.27)–(10.29), we obtain

$$(\sigma^f)^2 = \frac{1}{2(F_{22} - F_{23})}. \quad (10.30)$$

[5] S. W. Tsai and H. T. Hahn, *Introduction to Composite Materials*. Technomic, Lancester, Pennsylvania, 1980, p. 286.

Next, we apply only the shear stress τ_{23} (Fig. 10.8, bottom left). At failure the value of the shear stress is $\tau_{23} = \tau_{23}^{\mathrm{f}}$. Equation (10.12) now yields

$$F_{44}\left(\tau_{23}^{\mathrm{f}}\right)^2 = 1. \tag{10.31}$$

We evaluate F_{44} by observing that (a) the biaxial loading (Fig. 10.8, top left) is equivalent to a shear loading τ^{45} in the 45-degree direction (Fig. 10.8, top right), and (b) in the x_2–x_3 isotropy plane the magnitude of the failure shear stress is the same in every direction (Fig. 10.8, bottom). Consequently, at failure, the shear stress is $\tau_{23}^{\mathrm{f}} = \sigma^{\mathrm{f}}$. By substituting σ^{f} for τ_{23}^{f} in Eq. (10.31) and by using Eq. (10.30), we obtain

$$F_{44} = 2\left(F_{22} - F_{23}\right). \tag{10.32}$$

With these simplifications, for a transversely isotropic material the quadratic failure criterion (Eq. 10.11) becomes

$$\begin{aligned} F_1\sigma_1 + F_2\left(\sigma_2 + \sigma_3\right) + F_{11}\sigma_1^2 + F_{22}\left(\sigma_2^2 + \sigma_3^2\right) \\ + 2\left(F_{22} - F_{23}\right)\tau_{23}^2 + F_{66}\left(\tau_{13}^2 + \tau_{12}^2\right) + \\ 2F_{12}\left(\sigma_1\sigma_2 + \sigma_1\sigma_3\right) + 2F_{23}\sigma_2\sigma_3 < 1. \end{aligned} \tag{10.33}$$

The noninteraction strength parameters in terms of the strengths are summarized in Table 10.2 (page 417); the interaction strength parameters are given by Eq. (10.26). The strength parameters depend on the strengths. The tests for determining the required strengths s_1^+, s_1^-, s_2^+, s_2^-, s_{12} are illustrated in Figure 10.9.

10.1.3 Isotropic Material

Isotropic materials have an infinite number of symmetry planes, and the strength parameters given in Eqs. (10.9) and (10.10) are zero. In addition, because each symmetry plane is isotropic, the subscripts 1, 2, and 3 are interchangeable. This results in

$$F_1 = F_2 = F_3 \qquad F_{11} = F_{22} = F_{33} \qquad F_{23} = F_{13} = F_{12}. \tag{10.34}$$

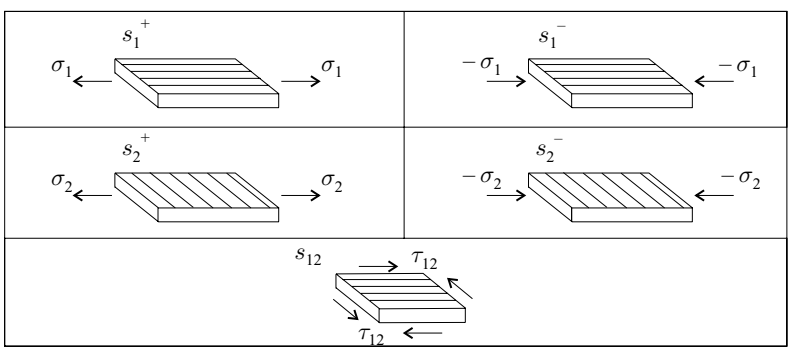

Figure 10.9: Tests to determine the strengths of a transversely isotropic material.

Similarly, $s_{12} = s_{13} = s_{23}$, and from Table 10.2 we have

$$F_{44} = F_{55} = F_{66}, \tag{10.35}$$

where F_{44} is given by Eq. (10.32). With the strength parameters given in Eqs. (10.34) and (10.35), the failure criterion (Eq. 10.11) becomes

$$F_1(\sigma_1 + \sigma_2 + \sigma_3) + F_{11}\left(\sigma_1^2 + \sigma_2^2 + \sigma_3^2\right) + 2(F_{11} - F_{12})\left(\tau_{23}^2 + \tau_{13}^2 + \tau_{12}^2\right) + 2F_{12}(\sigma_1\sigma_2 + \sigma_1\sigma_3 + \sigma_2\sigma_3) < 1. \tag{10.36}$$

Let us assume now that the compressive and tensile failure strengths are equal ($s_1^+ = s_1^-$). With this assumption, F_1 is zero (Table 10.2)

$$F_1 = 0. \tag{10.37}$$

Furthermore, let us approximate the interaction strength parameter by the expression given in Eq. (10.26) as follows:

$$F_{12} = -\frac{1}{2}\sqrt{F_{11}F_{22}} = -\frac{1}{2}F_{11}. \tag{10.38}$$

By substituting Eqs. (10.38) and (10.37) into Eq. (10.36) and by noting that $F_{11} = 1/(s_1^+)^2$, we obtain

$$\sqrt{\sigma_1^2 + \sigma_2^2 + \sigma_3^2 - \sigma_1\sigma_2 - \sigma_1\sigma_3 - \sigma_2\sigma_3 + 3\left(\tau_{23}^2 + \tau_{13}^2 + \tau_{12}^2\right)} < s_1^+. \tag{10.39}$$

This is identical to the von Mises quadratic failure criterion.[6]

10.1.4 Plane-Strain and Plane-Stress Conditions

Under plane-strain condition the equations and the parameters given in Sections 10.1.1–10.1.3 apply.

Under plane-stress condition (where in the x_1–x_2 plane $\sigma_3 = 0, \tau_{23} = 0, \tau_{13} = 0$, see Fig. 2.28) the quadratic failure criterion is simplified. For orthotropic materials and for transversely isotropic materials with x_1 normal to the plane of isotropy, Eqs. (10.12) and (10.33) become

$$F_1\sigma_1 + F_2\sigma_2 + F_{11}\sigma_1^2 + F_{22}\sigma_2^2 + F_{66}\tau_{12}^2 + 2F_{12}\sigma_1\sigma_2 < 1. \tag{10.40}$$

For isotropic materials, Eq. (10.36) reduces to

$$F_1(\sigma_1 + \sigma_2) + F_{11}\left(\sigma_1^2 + \sigma_2^2\right) + 2(F_{11} - F_{12})\tau_{12}^2 + 2F_{12}\sigma_1\sigma_2 < 1. \tag{10.41}$$

The strength parameters and the strengths required for the quadratic failure criteria are summarized in Tables 10.4 and 10.5.

[6] N. E. Dowling, *Mechanical Behavior of Materials*. Prentice-Hall, Englewood Cliffs, New Jersey, 1993, p. 245.

Table 10.4. The strength parameters appearing in the quadratic failure criterion for an orthotropic (Eq. 10.11), transversely isotropic (Eq. 10.33), and isotropic material (Eq. 10.36).

Three-dimensional stresses or plane-strain condition

Orthotropic	F_1	F_2	F_3	F_{11}	F_{22}	F_{33}	F_{44}	F_{55}	F_{66}	F_{12}	F_{13}	F_{23}
Transversely isotropic	F_1	F_2		F_{11}	F_{22}				F_{66}	F_{12}		F_{23}
Isotropic	F_1			F_{11}						F_{12}		

Plane-stress condition

Orthotropic or transversely isotropic	F_1	F_2		F_{11}	F_{22}			F_{66}	F_{12}		
Isotropic	F_1			F_{11}					F_{12}		

10.1.5 Proportional Loading – Stress Ratio

We consider a part subjected to a load set $L_1, L_2, \ldots, L_i$. Let us increase (or decrease) the loads proportionally by a factor of $\widetilde{R}$ until failure occurs (Fig. 10.10):

$$L_1^{\mathrm{f}} = \widetilde{R}L_1 \qquad L_2^{\mathrm{f}} = \widetilde{R}L_2 \quad \ldots. \quad L_i^{\mathrm{f}} = \widetilde{R}L_i. \tag{10.42}$$

When the part behaves in a linearly elastic manner, the stresses also increase (or decrease) proportionally. Consequently, each stress component increases (or decreases) by the same proportion until failure occurs. This procedure is expressed as

$$\begin{aligned} \sigma_1^{\mathrm{f}} &= \widetilde{R}\sigma_1 \qquad \tau_{23}^{\mathrm{f}} = \widetilde{R}\tau_{23} \\ \sigma_2^{\mathrm{f}} &= \widetilde{R}\sigma_2 \qquad \tau_{13}^{\mathrm{f}} = \widetilde{R}\tau_{13} \\ \sigma_3^{\mathrm{f}} &= \widetilde{R}\sigma_3 \qquad \tau_{12}^{\mathrm{f}} = \widetilde{R}\tau_{12}. \end{aligned} \tag{10.43}$$

The superscript f refers to the stress components on the failure surface, and $\widetilde{R}$ is the factor (called stress ratio) by which each load (and correspondingly each stress component) is multiplied such that the failure surface is reached; $\widetilde{R}$ is illustrated in Figure 10.11 for linearly elastic materials. No failure occurs when $\widetilde{R} > 1$, and

Table 10.5. The strengths required for evaluating the noninteraction strength parameters (see Tables 10.2 and 10.4)

Three-dimensional stresses or plane-strain condition

Orthotropic	s_1^+	s_1^-	s_2^+	s_2^-	s_3^+	s_3^-	s_{12}	s_{13}	s_{23}
Transversely isotropic	s_1^+	s_1^-	s_2^+	s_2^-			s_{12}		
Isotropic	s_1^+	s_1^-							

Plane-stress condition

Orthotropic or transversely isotropic	s_1^+	s_1^-	s_2^+	s_2^-	s_{12}	
Isotropic	s_1^+	s_1^-				

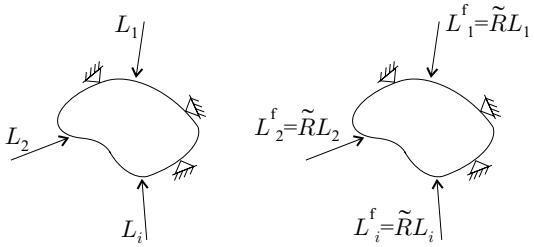

Figure 10.10: Proportional loading.

failure occurs when $\widetilde{R} \leq 1$:

$$\begin{array}{ll} \widetilde{R} > 1 & \text{no failure} \\ \widetilde{R} \leq 1 & \text{failure.} \end{array} \tag{10.44}$$

By substituting Eq. (10.43) into Eq. (10.12), we observe that the quadratic failure criterion for orthotropic materials becomes

$$\begin{aligned} &\widetilde{R}\left(F_1\sigma_1 + F_2\sigma_2 + F_3\sigma_3\right) + \\ &\widetilde{R}^2\left(F_{11}\sigma_1^2 + F_{22}\sigma_2^2 + F_{33}\sigma_3^2 + F_{44}\tau_{23}^2 + F_{55}\tau_{13}^2 + F_{66}\tau_{12}^2\right) + \\ &2\widetilde{R}^2\left(F_{12}\sigma_1\sigma_2 + F_{13}\sigma_1\sigma_3 + F_{23}\sigma_2\sigma_3\right) = 1. \end{aligned} \tag{10.45}$$

Whether or not failure occurs is indicated by the value of the stress ratio; $\widetilde{R}$ is given by the solution of Eq. (10.45) as follows:

$$\widetilde{R} = \frac{-b + \sqrt{b^2 + 4a}}{2a}. \tag{10.46}$$

Only the positive sign is applied in front of the square root because $\widetilde{R}$, by definition, is positive. The coefficients a and b are given in Table 10.6 for orthotropic, transversely isotropic, and isotropic materials.

Under plane-strain condition the expressions in Table 10.6 apply.

Under plane-stress condition, in the x_1–x_2 plane, σ_3, τ_{23}, τ_{13} are zero ($\sigma_3 = 0$, $\tau_{23} = 0$, and $\tau_{13} = 0$, Fig. 2.28). By setting these stresses equal to zero in Table 10.6, we obtain the a and b parameters listed in Table 10.7.

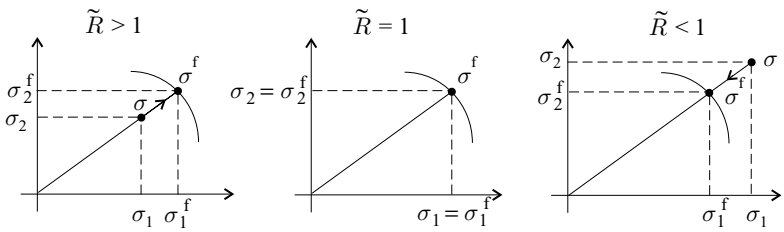

Figure 10.11: Representation of the failure surface when only σ_1 and σ_2 stresses are applied ($\widetilde{R} = \sigma_1^f/\sigma_1 = \sigma_2^f/\sigma_2$).

Table 10.6. The stress ratio $\widetilde{R}$

Material	*a*	*b*
Orthotropic	$F_{11}\sigma_1^2 + F_{22}\sigma_2^2 + F_{33}\sigma_3^2 + F_{44}\tau_{23}^2 + F_{55}\tau_{13}^2 + F_{66}\tau_{12}^2 + 2(F_{12}\sigma_1\sigma_2 + F_{13}\sigma_1\sigma_3 + F_{23}\sigma_2\sigma_3)$	$F_1\sigma_1 + F_2\sigma_2 + F_3\sigma_3$
Transversely isotropic	$F_{11}\sigma_1^2 + F_{22}(\sigma_2^2 + \sigma_3^2) + 2(F_{22} - F_{23})\tau_{23}^2 + F_{66}(\tau_{13}^2 + \tau_{12}^2) + 2F_{12}(\sigma_1\sigma_2 + \sigma_1\sigma_3) + 2F_{23}\sigma_2\sigma_3$	$F_1\sigma_1 + F_2(\sigma_2 + \sigma_3)$
Isotropic	$F_{11}(\sigma_1^2 + \sigma_2^2 + \sigma_3^2) + 2(F_{11} - F_{12})(\tau_{23}^2 + \tau_{13}^2 + \tau_{12}^2) + 2F_{12}(\sigma_1\sigma_2 + \sigma_1\sigma_3 + \sigma_2\sigma_3)$	$F_1(\sigma_1 + \sigma_2 + \sigma_3)$

$$\widetilde{R} = \frac{-b+\sqrt{b^2+4a}}{2a}$$

10.2 "Maximum Stress" Failure Criterion

Frequently, for orthotropic materials and for transversely isotropic materials under plane-stress condition, a so-called "maximum stress" criterion is used. In applying this criterion we use the x_1, x_2, x_3 coordinate system aligned with the direction of orthotropy (Fig. 2.12, left). The normal stresses in the x_1, x_2, x_3 directions and the shear stresses in the x_1–x_2, x_3–x_1, x_2–x_3 planes are compared with the corresponding strengths. Failure does not occur if none of the stresses exceeds the strengths.

For an orthotropic material, no failure occurs when all of the following conditions are met:

$$\begin{aligned} -s_1^- < \sigma_1 < s_1^+ \qquad & |\tau_{23}| < s_{23} \\ -s_2^- < \sigma_2 < s_2^+ \qquad & |\tau_{13}| < s_{13} \\ -s_3^- < \sigma_3 < s_3^+ \qquad & |\tau_{12}| < s_{12}. \end{aligned} \tag{10.47}$$

For a transversely isotropic material under plane-stress condition, no failure occurs when all of the following conditions are met:

$$-s_1^- < \sigma_1 < s_1^+ \qquad -s_2^- < \sigma_2 < s_2^+ \qquad |\tau_{12}| < s_{12}, \tag{10.48}$$

Table 10.7. The stress ratio $\widetilde{R}$ under plane-stress condition

Material	*a*	*b*
Orthotropic or transversely isotropic	$F_{11}\sigma_1^2 + F_{22}\sigma_2^2 + F_{66}\tau_{12}^2 + 2F_{12}\sigma_1\sigma_2$	$F_1\sigma_1 + F_2\sigma_2$
Isotropic	$F_{11}(\sigma_1^2 + \sigma_2^2) + 2(F_{11} - F_{12})\tau_{12}^2 + 2F_{12}\sigma_1\sigma_2$	$F_1(\sigma_1 + \sigma_2)$

$$\widetilde{R} = \frac{-b+\sqrt{b^2+4a}}{2a}$$

where s_i^+ and s_i^- are the tensile and compressive strengths in the i direction and s_{ij}^+ are the shear strengths in the ij $(i, j = 1, 2, 3)$ plane (Table 10.1, page 417).

Two important points are to be made here as follows:

1. The "maximum stress" criterion differs from the quadratic failure criterion.
2. The "maximum stress" failure criterion for composites differs from the maximum (normal or shear) stress criterion used for isotropic materials. The reason is that for isotropic materials the maximum (normal or shear) stress failure criterion is based on the maximum values of the stresses at a point. On the other hand, for composite materials the "maximum stress" failure criterion is based on the stress components in the orthotropy directions where the stresses are not necessarily the highest.

Despite the aforementioned shortcomings, the maximum stress criterion for composites (Eqs. 10.47, 10.48) has the advantage that it does not require knowledge of the interaction strength parameters.

10.3 "Maximum Strain" Failure Criterion

Frequently, for orthotropic materials and for transversely isotropic materials under plane-stress condition, a so-called maximum strain criterion is used. In applying this criterion we use the x_1, x_2, x_3 coordinate system aligned with the direction of orthotropy (Fig. 2.12, left). The normal strains in the x_1, x_2, x_3 directions and the shear strains in the x_1–x_2, x_3–x_1, x_2–x_3 planes are compared with the corresponding maximum allowable strains. Failure does not occur if none of the strains exceeds the allowable strains.

For an orthotropic material, no failure occurs when all of the following conditions are met:

$$\begin{aligned} -\eta_1^- < \epsilon_1 < \eta_1^+ \qquad & |\gamma_{23}| < \eta_{23}^+ \\ -\eta_2^- < \epsilon_2 < \eta_2^+ \qquad & |\gamma_{13}| < \eta_{13}^+ \\ -\eta_3^- < \epsilon_3 < \eta_3^+ \qquad & |\gamma_{12}| < \eta_{12}^+. \end{aligned} \tag{10.49}$$

For a transversely isotropic material, under plane-stress condition no failure occurs when all of the following conditions are met:

$$-\eta_1^- < \epsilon_1 < \eta_1^+ \qquad -\eta_2^- < \epsilon_2 < \eta_2^+ \qquad |\gamma_{12}| < \eta_{12}^+, \tag{10.50}$$

where η_i^+ and η_i^- are the allowable tensile and compressive strains in the x_i direction, and η_{ij}^+ are the allowable shear strains in the x_i–x_j $(i, j = 1, 2, 3)$ planes.

In general, the strain components above do not necessarily correspond to the maximum strain at the point. Therefore, this is not a true maximum strain failure criterion and is not equivalent to the maximum strain failure criterion for isotropic

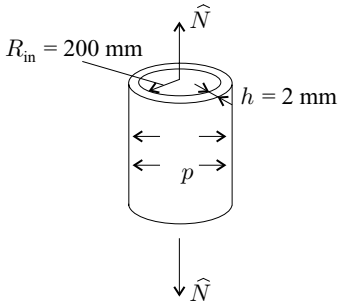

Figure 10.12: The cylinder subjected to internal pressure and axial load in Example 10.1.

materials, where failure is based on the maximum value of the strain components at the point.

Furthermore, the "maximum strain" (Eq. 10.50) failure criterion above is not equivalent to the "maximum stress" failure criterion (Eq. 10.48).

10.1 Example. *A cylinder (inner radius $R_{in} = 0.2$ m, and wall thickness $h = 0.002$ m) is made of woven glass epoxy. The material properties are given in Tables C.3 and C.4 (page 466). The cylinder is subjected to an axial load $\widehat{N} = 500\,000$ N and to an internal pressure $p = 2\,000\,000$ N/m^2 (Fig. 10.12). Determine the stress ratio $\widetilde{R}$.*

Solution. The radius of the reference surface, chosen as the midsurface, is

$$R = R_{\text{in}} + h/2 = 0.201 \text{ m}. \tag{10.51}$$

Using the membrane theory of shells, we determine that the membrane forces are (Eq. 8.11, with $p \equiv p_z$)

$$N_x = \frac{\widehat{N}}{2\pi R} = 395\,908 \frac{\text{N}}{\text{m}} \qquad N_y = pR = 402\,000 \frac{\text{N}}{\text{m}} \qquad N_{xy} = \frac{\widehat{T}}{2\pi R^2} = 0. \tag{10.52}$$

The stresses in the wall are

$$\begin{aligned} \sigma_x &= \frac{N_x}{h} = 197.95 \times 10^6 \frac{\text{N}}{\text{m}^2} \\ \sigma_y &= \frac{N_y}{h} = 201.00 \times 10^6 \frac{\text{N}}{\text{m}^2} \\ \tau_{xy} &= \frac{N_{xy}}{h} = 0. \end{aligned} \tag{10.53}$$

The wall of the cylinder consists of a single layer. The coordinates of this layer are x_1, x_2, x_3, and they coincide with the x, y, z coordinates of the cylinder (Fig. 10.12). Thus, the stresses in the layer are

$$\begin{aligned} \sigma_1 &= 197.95 \times 10^6 \frac{\text{N}}{\text{m}^2} \\ \sigma_2 &= 201.00 \times 10^6 \frac{\text{N}}{\text{m}^2} \\ \tau_{12} &= 0. \end{aligned} \tag{10.54}$$

With the strengths listed in Table C.4 ($s_1^+ = 367$ MPa, $s_1^- = 549$ MPa, $s_2^+ = 367$ MPa, $s_2^- = 549$ MPa, $s_{12} = 97$ MPa), the required strength parameters are (Table 10.2, page 417 and Eq. 10.26)

$$\begin{aligned} F_1 &= \frac{1}{s_1^+} - \frac{1}{s_1^-} = 903 \times 10^{-12} \qquad F_{11} = \frac{1}{s_1^+ s_1^-} = 4.96 \times 10^{-18} \\ F_2 &= \frac{1}{s_2^+} - \frac{1}{s_2^-} = 903 \times 10^{-12} \qquad F_{22} = \frac{1}{s_2^+ s_2^-} = 4.96 \times 10^{-18} \\ F_{66} &= \frac{1}{(s_{12})^2} = 106 \times 10^{-18} \qquad F_{12} = -\frac{1}{2}\sqrt{F_{11}F_{22}} = -2.48 \times 10^{-18}. \end{aligned} \tag{10.55}$$

The stress ratio from Table 10.7 (page 425) is

$$a = F_{11}\sigma_1^2 + F_{22}\sigma_2^2 + F_{66}\tau_{12}^2 + 2F_{12}\sigma_1\sigma_2 = 0.1975 \tag{10.56}$$

$$b = F_1\sigma_1 + F_2\sigma_2 = 0.3604 \tag{10.57}$$

$$\widetilde{R} = \frac{-b + \sqrt{b^2 + 4a}}{2a} = 1.52 > 1, \tag{10.58}$$

where $\widetilde{R}$ is greater than unity and the cylinder does not fail.

Next, we establish the failure envelope. At failure the Tsai–Wu criterion is (see Eqs. 10.40 and 10.3)

$$F_1\sigma_1^{\mathrm{f}} + F_2\sigma_2^{\mathrm{f}} + F_{11}\left(\sigma_1^{\mathrm{f}}\right)^2 + F_{22}\left(\sigma_2^{\mathrm{f}}\right)^2 + F_{66}\left(\tau_{12}^{\mathrm{f}}\right)^2 + 2F_{12}\sigma_1^{\mathrm{f}}\sigma_2^{\mathrm{f}} = 1, \tag{10.59}$$

where the superscript f refers to the stresses at failure, which are (Eqs. 10.52 and 10.53)

$$\begin{aligned} \sigma_1^{\mathrm{f}} &= \frac{N_x}{h} = \frac{\widehat{N}^{\mathrm{f}}}{2\pi Rh} = 395.9\widehat{N}^{\mathrm{f}} \\ \sigma_2^{\mathrm{f}} &= \frac{N_y}{h} = \frac{p^{\mathrm{f}}R}{h} = 100.5p^{\mathrm{f}} \\ \tau_{12}^{\mathrm{f}} &= \frac{N_{xy}}{h} = \frac{\widehat{T}}{2\pi R^2 h} = 0, \end{aligned} \tag{10.60}$$

where $\widehat{N}^{\mathrm{f}}$ and p^{f} are the applied loads at failure. In terms of $\widehat{N}^{\mathrm{f}}$ and p^{f}, Eq. (10.59) gives

$$\begin{aligned} 3.58 \times 10^{-7}\widehat{N}^{\mathrm{f}} + 9.08 \times 10^{-8}p^{\mathrm{f}} + 7.78 \times 10^{-13}(\widehat{N}^{\mathrm{f}})^2 + \\ 5.01 \times 10^{-14}(p^{\mathrm{f}})^2 - 1.97 \times 10^{-13}\widehat{N}^{\mathrm{f}}p^{\mathrm{f}} = 1. \end{aligned}$$

The failure envelope along which the $\widehat{N}^{\mathrm{f}}$ and p^{f} values satisfy this condition is plotted in Figure 10.13.

The "maximum stress" failure criterion is (Eq. 10.47)

$$-s_1^- < \sigma_1 < s_1^+ \tag{10.61}$$

$$-s_2^- < \sigma_2 < s_2^+. \tag{10.62}$$

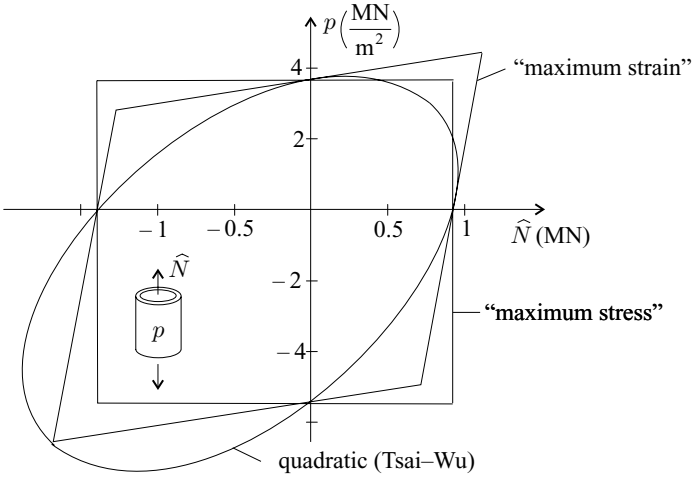

Figure 10.13: The "maximum stress," "maximum strain," and the quadratic (Tsai–Wu) failure envelopes for the cylinder in Example 10.1.

The value of $\sigma_1 = 197.95$ MPa is between $-s_1^- = -549$ MPa and $s_1^+ = 367$ MPa, and $\sigma_2 = 201$ MPa is between $-s_2^- = -549$ MPa and $s_2^+ = 367$ MPa. Hence, the cylinder does not fail.

To establish the failure envelope, we note that failure occurs when any of the following conditions are met:

$$\begin{aligned} -s_1^- = -549 = \sigma_1^{\text{f}} = 395.9\widehat{N}^{\text{f}} \qquad & s_1^+ = 367 = \sigma_1^{\text{f}} = 395.9\widehat{N}^{\text{f}} \\ -s_2^- = -549 = \sigma_2^{\text{f}} = 100.5p^{\text{f}} \qquad & s_2^+ = 367 = \sigma_2^{\text{f}} = 100.5p^{\text{f}}. \end{aligned} \tag{10.63}$$

The failure envelope represented by these equations is included in Figure 10.13.

The "maximum strain" failure criterion is (Eq. 10.49)

$$\begin{aligned} -\eta_1^- < \epsilon_1 < \eta_1^+ \\ -\eta_2^- < \epsilon_2 < \eta_2^+. \end{aligned} \tag{10.64}$$

With the engineering constants $E_1 = E_2 = 29.7 \times 10^9$ N/m^2 (Table C.3, page 466), the maximum allowable strains are

$$\begin{aligned} \eta_1^- = \frac{s_1^-}{E_1} = 0.0185 \qquad & \eta_1^+ = \frac{s_1^+}{E_1} = 0.0124 \\ \eta_2^- = \frac{s_2^-}{E_2} = 0.0185 \qquad & \eta_2^+ = \frac{s_2^+}{E_2} = 0.0124. \end{aligned} \tag{10.65}$$

With S_{ij} given in Table 2.7 (page 15), the strain–stress relationships are (Eq. 2.132)

$$\begin{Bmatrix} \epsilon_1 \\ \epsilon_2 \\ \gamma_{12} \end{Bmatrix} = \begin{bmatrix} \frac{1}{E_1} & -\frac{\nu_{21}}{E_2} & 0 \\ -\frac{\nu_{12}}{E_1} & \frac{1}{E_2} & 0 \\ 0 & 0 & \frac{1}{G_{12}} \end{bmatrix} \begin{Bmatrix} \sigma_1 \\ \sigma_2 \\ \tau_{12} \end{Bmatrix}. \tag{10.66}$$

The engineering constants are $E_1 = E_2 = 29.7 \times 10^9$ N/m^2, $G_{12} = 5.3 \times 10^9$ N/m^2, $\nu_{12} = 0.17$ (Table C.3). Thus, we have

$$\begin{Bmatrix} \epsilon_1 \\ \epsilon_2 \\ \gamma_{12} \end{Bmatrix} = \begin{bmatrix} 33.67 & -5.72 & 0 \\ -5.72 & 33.67 & 0 \\ 0 & 0 & 188.68 \end{bmatrix} \times 10^{-12} \begin{Bmatrix} 197.95 \\ 201.00 \\ 0 \end{Bmatrix} \times 10^6$$
$$= \begin{Bmatrix} 0.005\,51 \\ 0.005\,63 \\ 0 \end{Bmatrix}. \tag{10.67}$$

The value $\epsilon_1 = 0.005\,51$ is between $-\eta_1^- = -0.018\,5$ and $\eta_1^+ = 0.012\,4$, and $\epsilon_2 = 0.005\,63$ is between $-\eta_2^- = -0.018\,5$ and $\eta_2^+ = 0.012\,4$. Therefore, the cylinder does not fail.

To establish the failure envelope, we note that failure occurs when any of the following conditions is met:

$$\begin{aligned} -\eta_1^- &= \epsilon_1^{\mathrm{f}} \quad \eta_1^+ = \epsilon_1^{\mathrm{f}} \\ -\eta_2^- &= \epsilon_2^{\mathrm{f}} \quad \eta_2^+ = \epsilon_2^{\mathrm{f}}, \end{aligned} \tag{10.68}$$

where ϵ_1^{f} and ϵ_2^{f} are the strains at failure, which, in terms of $\widehat{N}^{\mathrm{f}}$ and p^{f}, are (Eqs. 10.66 and 10.60)

$$\begin{aligned} \epsilon_1^{\mathrm{f}} &= (13.3\widehat{N}^{\mathrm{f}} - 0.575p^{\mathrm{f}}) \times 10^{-9} \\ \epsilon_2^{\mathrm{f}} &= (-2.27\widehat{N}^{\mathrm{f}} + 3.38p^{\mathrm{f}}) \times 10^{-9}. \end{aligned} \tag{10.69}$$

From Eqs. (10.65), (10.68), and (10.69) we have

$$\begin{aligned} -0.0185 \times 10^9 &= 13.3\widehat{N}^{\mathrm{f}} - 0.575p^{\mathrm{f}} \qquad 0.0124 \times 10^9 = 13.3\widehat{N}^{\mathrm{f}} - 0.575p^{\mathrm{f}} \\ -0.0185 \times 10^9 &= -2.27\widehat{N}^{\mathrm{f}} + 3.38p^{\mathrm{f}} \qquad 0.0124 \times 10^9 = -2.27\widehat{N}^{\mathrm{f}} + 3.38p^{\mathrm{f}}. \end{aligned} \tag{10.70}$$

The failure envelope represented by these equations is included in Figure 10.13.

Figure 10.13 shows that the failure envelopes are markedly different for the quadratic (Tsai–Wu), the "maximum stress," and the "maximum strain" failure criteria. Thus, although in this example all three failure criteria indicate that there is no failure, there may be conditions under which they give contradictory results.

10.4 Plate with a Hole or a Notch

The quadratic, maximum stress, and maximum strain failure criteria are inapplicable when failure is initiated by localized disturbances such as imperfections, cracks, holes, notches, or free edges. If any of these criteria were evaluated using the stresses near the disturbance (where the stresses are high), the criteria would underestimate the failure load. On the other hand, if the criteria were evaluated using the stresses in the farfield (where the stresses are significantly lower than the nearfield stresses), the criteria would overestimate the failure load. To

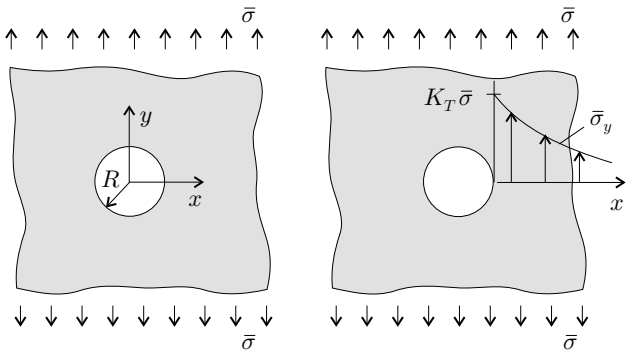

Figure 10.14: Unidirectionally loaded plate contaning a circular hole and the average stress distribution along the x-axis near the hole.

predict the failure in the presence of a disturbance we would need an understanding of the fracture behavior of the material and appropriate fracture models. To date, there is no simple, comprehensive model that describes failure of different composite systems largely because different systems exhibit different damage mechanisms and failure modes. One model, which is applicable in engineering design, is Whitney and Nuismer's[7,8] model for predicting failure of laminates with local stress concentrations. In the following we illustrate the concept underlying this model via the failure of laminates containing a circular hole or a notch.

10.4.1 Plate with a Circular Hole

Let us consider a large plate containing a circular hole of radius R (Fig. 10.14, left). The plate is subjected to a uniformly distributed average tensile stress $\overline{\sigma}$. Under the action of this stress the through-the-thickness average of the normal stress along the x axis is $\overline{\sigma}_y$ (Fig. 10.14, right).

Whitney and Nuismer proposed two failure criteria, one referred to as the point-stress the other as the average stress criterion.

According to the *point stress criterion*, failure occurs when, at a fixed distance d_0 from the hole along the x-axis (Fig. 10.15), $\overline{\sigma}_y$ is equal to or greater than the stress at failure of the "solid" plate (i.e., the plate *without* the hole),

$$\overline{\sigma}_y\,(R+d_0,0) \geq \overline{\sigma}_0^{\mathrm{f}} \qquad \text{failure}, \tag{10.71}$$

where $\overline{\sigma}_0^{\mathrm{f}}$ is the strength of the solid plate (Fig. 10.16).

According to the *average stress criterion*, failure occurs when the stress $\overline{\sigma}_y$, averaged over a fixed distance a_0 along the x-axis, is equal to or greater than the

[7] J. M. Whitney and R. J. Nuismer, Stress Fracture Criteria for Laminated Composites Containing Stress Concentrations. *Journal of Composite Materials*, Vol. 8, 253–265, 1974.

[8] R. J. Nuismer and J. M. Whitney, Uniaxial Failure of Composite Laminates Containing Stress Concetrations. In: *Fracture Mechanics of Composites*. ASTM STP 593, American Society for Testing and Materials, Philadelphia, 1975, pp. 117–142.

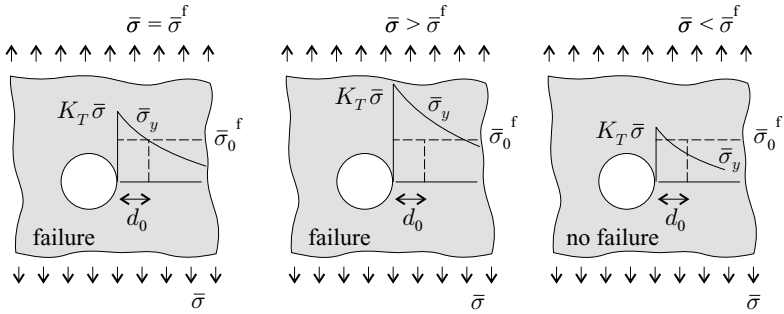

Figure 10.15: Illustration of the failure of a plate with a circular hole according to the point stress failure criterion.

failure stress of the "solid" plate:

$$\frac{1}{a_0}\int_R^{R+a_0} \overline{\sigma}_y\,(x,0)\,dx \geq \overline{\sigma}_0^{\mathrm{f}} \qquad \text{failure.} \tag{10.72}$$

To apply either of the criteria above, the strength $\overline{\sigma}_0^{\mathrm{f}}$ of the solid plate (Fig. 10.16) and the stress distribution $\overline{\sigma}_y$ (Fig. 10.15) must be known. The strength is to be obtained by tests. The stress distribution must be determined numerically.

Orthotropic plate. For orthotropic plates (with the x- and y-axes in the directions of orthotropy) the stress distribution along the x-axis is given by Eq. (4.305). With the definitions $\overline{\sigma}_y = N_y/h$ and $\overline{\sigma} = N_y^{\infty}/h$, we write Eq. (4.305) as

$$\overline{\sigma}_y\,(x,0) = \frac{\overline{\sigma}}{2}\left\{2 + \left(\frac{R}{x}\right)^2 + 3\left(\frac{R}{x}\right)^4 - (K_T - 3)\left[5\left(\frac{R}{x}\right)^6 - 7\left(\frac{R}{x}\right)^8\right]\right\}, \tag{10.73}$$

where $\overline{\sigma}$ is the applied uniform tensile stress (Fig. 10.14) and K_T is the stress intensity factor ($K_T = \overline{\sigma}_y(R,0)/\overline{\sigma}$). From Eq. (4.304), K_T is

$$K_T = 1 + \sqrt{\frac{2}{A_{11}}\left(\sqrt{A_{11}A_{22}} - A_{12} + \frac{A_{11}A_{22} - A_{12}^2}{2A_{66}}\right)}, \tag{10.74}$$

where A_{ij} are the elements of the stiffness matrix in the x–y coordinate system (Eq. 3.20). At failure $\overline{\sigma}$ is denoted by $\overline{\sigma}^{\mathrm{f}}$ (Fig. 10.16). With this notation, Eqs. (10.71)

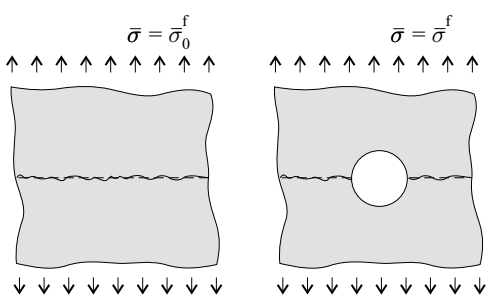

Figure 10.16: The applied stress at failure of a plate without and with the hole.

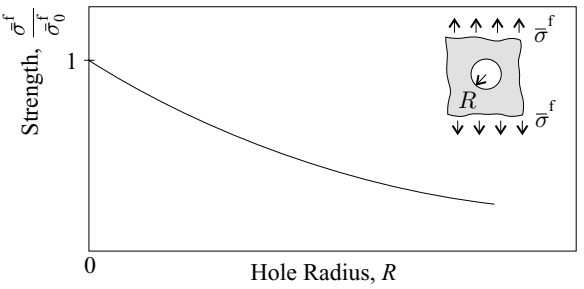

Figure 10.17: The strength of a composite plate with a hole as the function of the hole size.

and (10.73) yield

$$\frac{\overline{\sigma}^{\mathrm{f}}}{\overline{\sigma}_0^{\mathrm{f}}} = \frac{2}{2 + r^2 + 3r^4 - (K_T - 3)\,(5r^6 - 7r^8)} \qquad \begin{array}{l}\text{orthotropic plate}\\ \text{with hole.}\end{array} \tag{10.75}$$

The parameter r is defined as

$$r = \frac{R}{R + d_0}. \tag{10.76}$$

The expression using the average stress criterion is not given because Whitney and Nuismer have shown that the point stress and average stress criteria yield very similar results.

Equation (10.75) shows the hole size effect, which has also been observed experimentally: when subjected to tension, plates with larger holes have lower strengths than plates with smaller holes (Fig. 10.17). To explain this phenomenon, we observe that the high stresses in the vicinity of the hole are confined to a region that is narrower for smaller holes than for larger holes (Fig. 10.18). One possible explanation for the hole size effect is that, in this narrower region, there are fewer flaws (failure initiation sites) that could initiate damage growth, resulting in reduced strength.

It has also been argued that plates with smaller holes are stronger because stress gradients near the hole can better distribute for small holes (where the stress gradients are high) than for large holes (where the stress gradients are smaller).

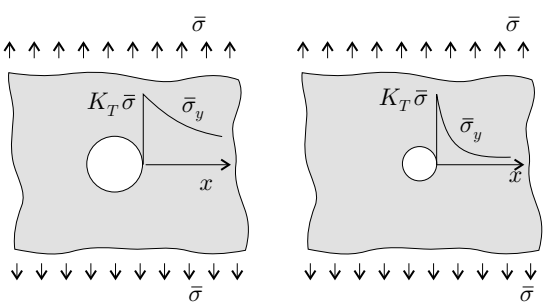

Figure 10.18: The stress distribution along the x-axis for two different hole sizes.

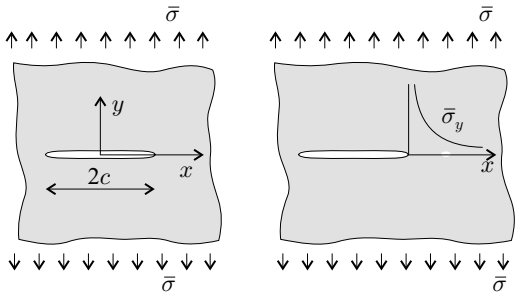

Figure 10.19: Unidirectionally loaded plate contaning a notch and the stress distribution along the x-axis near the notch.

10.4.2 Plate with a Notch

We now apply the Whitney–Nuismer point stress criterion to a large symmetric orthotropic plate containing a through-the-width notch of length $2c$ (Fig. 10.19, left). The notch is aligned with one of the orthotropy axes. When this plate is subjected to a uniform tensile stress $\overline{\sigma}$, the through-the-thickness average of the normal stress along the x-axis $\overline{\sigma}_y$ (Fig. 10.19, right) is given by Whitney and Nuismer[9] as

$$\overline{\sigma}_y(x, 0) = \frac{\overline{\sigma} x}{\sqrt{x^2 - c^2}}. \tag{10.77}$$

Substitution of Eq. (10.77) into Eq. (10.71) (R replaced by c) yields

$$\frac{\overline{\sigma}^{\mathrm{f}}}{\overline{\sigma}_0^{\mathrm{f}}} = \sqrt{1 - \left(\frac{c}{c + d_0}\right)^2} \qquad \begin{matrix}\text{plate} \\ \text{with notch.}\end{matrix} \tag{10.78}$$

The average stress criterion can be obtained similarly. It is not given here because it yields results similar to the point stress criterion.

10.4.3 Characteristic Length

The usefulness of the Whitney–Nuismer point stress and average stress failure criteria is predicated on the assumption that the characteristic lengths d_0 or a_0 are independent of the hole or notch size – at least for a given laminate made of a particular material system. In such a case, the characteristic lengths can be determined through one test for one hole or one notch size. Obviously, the model would be even more useful if the characteristic lengths were to remain constant for all laminates (layups) made of different types of fiber-reinforced composites. There is evidence that the values of the characteristic lengths do not vary appreciably

[9] J. M. Whitney and R. J. Nuismer, Stress Fracture Criteria for Laminated Composites Containing Stress Concentrations. *Journal of Composite Materials*, Vol. 8, 253–265, 1974.

over a wide range of conditions. For example, Nuismer and Whitney[10] have found that the values $d_0 = 1.0$ mm and $a_0 = 3.8$ mm fit the data for cross-ply and quasi-isotropic glass–epoxy and graphite epoxy laminates containing a circular hole or a notch well. Although the existing data are not all conclusive, the Whitney–Nuismer point stress and average stress criteria, together with the characteristic length values just cited, should be useful at least for the purpose of preliminary design.

[10] R. J. Nuismer and J. M. Whitney, Uniaxial Failure of Composite Laminates Containing Stress Concetrations. In: *Fracture Mechanics of Composites*. ASTM STP 593, American Society for Testing and Materials, Philadelphia, 1975, pp. 117–142.